PNAS

Supporting Information for
Mouse models of human multiple myeloma subgroups

Wiebke Winkler[a,b,c,d], Carlota Farré Díaz[a,b,c,d], Eric Blanc[e], Hanna Napieczynska[f], Patrick Langner[f], Marvin Werner[b,c,d], Barbara Walter[b,c,d,1], Brigitte Wollert-Wulf[b,c,d], Tomoharu Yasuda[a,2], Arnd Heuser[f], Dieter Beule[e], Stephan Mathas[b,c,d], Ioannis Anagnostopoulos[g], Andreas Rosenwald[g], Klaus Rajewsky[a,3], Martin Janz[b,c,d,3]

[a]Immune Regulation and Cancer, Max Delbrück Center for Molecular Medicine in the Helmholtz Association (MDC); Berlin, 13125, Germany

[b]Biology of Malignant Lymphomas, Max Delbrück Center for Molecular Medicine in the Helmholtz Association (MDC); Berlin, 13125, Germany

[c]Experimental and Clinical Research Center (ECRC), a cooperation between the Max Delbrück Center for Molecular Medicine in the Helmholtz Association and the Charité – Universitätsmedizin Berlin; Berlin, 13125, Germany

[d]Hematology, Oncology and Cancer Immunology, Charité – Universitätsmedizin Berlin; Berlin, 13125, Germany

[e]Core Unit Bioinformatics (CUBI), Charité – Universitätsmedizin Berlin, corporate member of Freie Universität Berlin and Humboldt-Universität zu Berlin, and Berlin Institute of Health; Berlin, 10117, Germany

[f]Animal Phenotyping, Max Delbrück Center for Molecular Medicine in the Helmholtz Association (MDC); Berlin, 13125, Germany

[g]Institute of Pathology, Universität Würzburg and Comprehensive Cancer Centre Mainfranken (CCCMF); Würzburg, 97080, Germany

[1]Present address: Stem Cell Aging Group, Regenerative Medicine Program, Bellvitge Institute for Biomedical Research (IDIBELL); Barcelona, 08908, Spain

[2]Present address: Department of Immunology, Graduate School of Biomedical and Health Sciences (Medicine), Hiroshima University; Hiroshima, 739-8511, Japan

[3]co-corresponding authors: Klaus Rajewsky and Martin Janz
Email: klaus.rajewsky@mdc-berlin.de; mjanz@mdc-berlin.de

This PDF file includes:

Supporting Information Materials and Methods

Flow cytometry and cell sorting. Red blood cells were lysed with Gey's solution and single cell suspensions from spleen and BM were stained with antibody conjugates (Table S5) in PBS, pH 7.2, supplemented with 3 % FCS and 1 mM EDTA. The samples were analyzed on an LSRFortessa (BD BioSciences) or sorted on a FACSAria (BD BioSciences). Plots were generated using FlowJo software (BD FlowJo, RRID:SCR_008520; v9.9.6). For the analysis of NIP+ GC B cells, NIP-BSA-APC was used as described (1).

B cell culture and TATCre treatment. Splenic B cells were enriched by CD43 depletion with magnetic anti-mouse CD43 microbeads (Miltenyi Biotech, Cat#130-049-801) according to the manufacturer's instructions. To remove the STOP cassette, transgenic B cells were transduced *ex vivo* with in-house generated TATCre recombinase (2) and cultured in the presence of recombinant mouse IL-4 (25 ng/mL, R&D, Cat#404-ML) and either LPS (20 µg/mL, Sigma, Cat#L2880) or anti-mouse CD40 (1 µg/mL, BioLegend, HM40-3, Cat#102908). For the confirmation of MMSET expression, B cells had to be differentiated into plasma cells using the 40LB feeder cell system and recombinant mouse IL-21 (10 ng/mL, Peprotech, Cat#210-21) (3).

Real-time PCR and Western blotting. BFP+ B or plasma cells were sorted, total RNA extracted using the RNeasy Mini kit (QIAGEN, Cat#74104) and cDNA synthesized using SuperScript II Reverse Transcriptase (Invitrogen, Cat#18064022). The quantitative PCR was done with SYBR Green, followed by analysis with the StepOnePlus System (Applied Biosystems). Samples were assayed in triplicates, and mRNA abundance was normalized to that of *Hprt*. For Western blot, whole cell extracts of sorted BFP+ B or plasma cells were prepared as previously described (4). The primary antibodies used are listed in Table S5.

Immunohistochemistry. For decalcification, femurs were incubated for 24 h in 0.4 M EDTA pH 7.4, followed by 24 h in 30 % sucrose solution (in PBS) under constant rotation at 4 °C. Spleen sections and decalcified bones were embedded in Tissue-Tek O.C.T. Compound (Sakura Cat#4583), stored at -80 °C and cryosectioned (7 µm thickness). For immunofluorescence staining, slides were fixed for 15 min in 100 % acetone, blocked for 30 min with 3 % BSA (in PBS), stained for 2 h with the antibody conjugates listed in Table S5 and then for 5 min with DAPI (eBioScience Cat# D1306). For HE staining, frozen sections from the femur and spleen were stained with hematoxylin and eosin (HE) according to the following protocol: the slides were immersed for 15 min in hemalaun solution followed by a 5 min rinse in tap water and a 5 min incubation in eosin solution. After short (5 sec) rinses in tap water followed by 100 % ethanol and xylene, the slides were mounted in a film coverslipper (Tissue-Tek-Film® Automated Coverslipper, Sakura Finetek USA) and evaluated in a blinded fashion, i.e., without knowledge of the genotypes. Immunofluorescence and HE stained sections were imaged with a BZ-9000 microscope (Keyence).

Enzyme-linked immuno assays, serum protein electrophoresis and immunofixation. Enzyme-linked immunosorbent assays (ELISAs), enzyme-linked immuno spot (ELISPOT) assays and serum protein electrophoresis were performed as described (1) with the minor change that for the ELISA of cohort mouse samples plates were coated with 1 µg/mL anti-IgM, anti-IgG or anti-IgA instead of anti-light chain antibodies. Immunofixation was done on 1:6 (for IgG) or 1:3 (for all other Ig isotypes) diluted serum samples according to the "Hydragel 4 IF Immunofixation" kit (Sebia, Cat# 4804) using mouse antisera listed in Table S5.

VDJ-PCR. Genomic DNA was prepared from sorted BFP+GFP+ CD138+TACI+ long bone-derived BM plasma cells (NucleoSpin Tissue, Macherey-Nagel, Cat#740952). Ighv gene rearrangements were PCR amplified using the KOD HotStart DNA polymerase (Novagen, Cat#71086) and forward primers specific for VHA, VHB, VHC, VHD, VHE, VHF, VHG (5) as well as a reverse primer in the J_H4 intron (6). Prominent fragments were cloned, sequenced and aligned against the NCBI database IgBLAST (http://www.ncbi.nlm.nih.gov/igblast/; RRID:SCR_002873) to determine $V_HD_HJ_H$ gene segment usage.

RNA-Sequencing. 2,000 (reporter+) CD138+TACI+ long bone-derived BM plasma cells from 8x Control, 4x Ccnd1, 4x MMSET, 8x Ikk2ca, 6x Ccnd1/Ikk2ca and 6x MMSET/IKk2ca aged cohort mice were sorted into 75 µL RLT buffer (supplemented with β-mercaptoethanol) and stored at -80 °C. Total RNA was extracted using the RNeasy Micro Kit (QIAGEN, Cat#74004), then cDNA was synthesized using SuperScript II reverse transcriptase (Invitrogen, Cat#18064022), an Oligo-dT_{30}VN and a TSO (template switching oligo), followed by full-length sequence-independent cDNA amplification using KAPA HiFi HotStart ready mix (Roche, Cat#KK2601) and an ISPCR oligo as described (7). Finally, cDNA libraries were prepared using the Nextera XT DNA library preparation kit (Illumina, Cat#15032350) employing tagmentation to add Nextera XT indexes (Illumina, Cat#15055293). Libraries were sequenced on a NovaSeq6000 instrument as single 150 bp reads with a depth of approximately 100 million reads per sample.

Bioinformatic analysis: GSEA and Ighv gene usage. The 36 sequenced libraries contained between 71.8 & 130.4 million reads (median 86.5 million reads). The reads were mapped on the GRCm38 genome (GENCODE m23 annotations) using salmon (8) version 1.3.0 in selective alignment mapping mode. The mapping rate was between 61.0 % and 68.9 % (median 64.7 %). Because of their high abundance, genes and pseudogenes from the IMGT repertoire (immunoglobulins, J chain gene and T-cell receptors) were excluded from the gene expression analysis. The gene expression was computed from the mapping on transcripts using the tximport bioconductor package (9). DESeq2 (10) was used to compute differential expression over all samples together. Normalized expression levels were obtained by variance-stabilization transformation. For the gene set enrichment analysis, an overview of the tested gene sets can be found in Table S6. The tested modules were derived from Tables 4 and 5 (11), Table S4 (12), Tables 3 and 4 (13) and all supplementary tables containing MM subgroup-specific gene lists (14),(15),(16). To compute the gene sets' statistical significance, the CERNO test from R package tmod (17),(18) was used. For the CERNO test, mouse genes were ranked according to the value of the differential expression statistic provided by the "results" function of DESeq2. For every gene set, the test was run in both directions (from up- to down-regulation, and from down- to up-regulation). The clusterProfiler biocondutor package (19) was used to produce the gene set enrichment plots. Gene symbols required by the functional analysis were obtained directly from the GENCODE annotations.
For the Ighv (immunoglobulin heavy chain variable region) gene usage analysis, due to the 129 genetic background of the Cγ1-cre allele (20), counts for the Ighv genes were obtained by mapping reads on the GRCm38 genome, augmented with Ighv transcripts from the 129S1/SvImJ genome (taken from the ENSEMBL 103 release). The mapping was done using salmon. Then, for each sample the counts aligning to an individual Ighv gene were normalized to all Ighv gene counts (i.e., by setting the sum of all Ighv gene reads to 100 %) and plotted as a pie chart.

Whole exome sequencing (WES). 1-2 x 10^5 BFP+GFP+ CD138+TACI+ and CD19- plasma cells were sorted from the spleens of four Ccnd1/Ikk2ca #3459 and four MMSET/Ikk2ca #3939 spleen cell recipient mice as well as from the spleen and long bone-derived BM of the two donor mice (Ccnd1/Ikk2ca #3459 and MMSET/Ikk2ca #3939). In addition, BFP-GFP- CD138-TACI-CD19- CD11b+CD11c+ myeloid cells were sorted from the BM of both donor mice as reference controls. Genomic DNA was isolated from sorted cells using the NucleoSpin Tissue, Mini kit for DNA from cells and tissue (Macherey-Nagel, #740952.250). The SureSelect Enzymatic Fragmention Kit (Agilent, #5191-6764) was employed to fragment the genomic DNA, followed by the preparation of adaptor-tagged DNA libraries using the SureSelect XT HS2 DNA Reagent Kit (Agilent, #G9984A). Mouse exons were enriched by the SureSelectXT CD Mouse All Exon V2, 16. Community Design Kit (Agilent, #5191-6693) and libraries were amplified and indexed using the SureSelect XT HS2 DNA Reagent Kit (Agilent, #G9984A). The libraries were sequenced on a NovaSeq6000 instrument as paired-end 100 bp reads.

Bioinformatic analysis: SNV and CNV analysis. The WES data was processed using fastp (21) version 0.23.2 to trim the first 5 nucleotides from both reads in read pairs and to remove read pairs displaying long poly-G, as these reads were deemed affected by truncated fragment sequences. Then the data was aligned to the mm10 mouse genome release using bwa-mem (22)

version 0.7.17 with default settings. Base quality re-calibration was applied using GATK (23) version 4.2.6.1. Somatic variant calling was carried out on donor and recipient plasma cell tumors using the sorted cells as a proxy for normal samples in normal/tumor pairs. A fairly conservative protocol was selected for somatic variant calls. Three different somatic variant calling softwares were used: Mutect2 (24) version 4.2.6.1, LoFreq (25) version 2.1.5 & MuSE (26) version 2.0. Somatic variant candidates were retained if they were found by all three callers and passed all callers' internal filters. These candidates were then filtered to remove loci with multiple alternative variants alleles, or supported by 10 or fewer reads in the output of at least one caller. Only Single Nucleotide Variants (SNVs) were used for further analysis. The callers were used with default parameters. Mutect2 was used without panel of normal (i.e. sorted BM myeloid cells), but with the merged SNPs variants from dbSNP (27) version 142 to estimate contamination. The LoFreq tools suite was used to include in the calling process mismatches & indels identified during mapping. CNVkit (28) version 0.9.9 was used for Copy Number Alteration (CNA) calling. CNVkit standard pipeline was applied with default parameters. A reference was built from all reference samples (i.e. myeloid cells sorted from the donor mice BM), after verification that they did not show obvious CNAs, which was done by comparing the sorted myeloid samples to a flat reference of neutral copy number.

Micro-Computed Tomographic (µCT) analysis. The bone scans were performed post mortem for tibiae and skulls for virtually all animals with rare exceptions. Mouse skulls and tibiae were scanned with a SkyScan 1276 scanner (Bruker, Belgium) using the vendor's software for image acquisition (v.1.4.0.0), the step-and-shoot mode, the source current of 200 µA and 360° acquisition. Tibiae were scanned using the source voltage of 55 kV, Al 0.5 mm filter, an exposure time of 640 ms, 0.1° rotation step, and 3 frame averages. The pixel size was 5.0 µm. The skulls were scanned with the source voltage of 100 kV, Cu 0.25 mm filter, exposure time of 645 ms, 0.2° rotation step, and 3 frame averages. The pixel size was 10.65 µm. The flat field correction was applied for all acquisitions. Image reconstruction was performed with NRecon (v.1.7.3.1, Bruker, Belgium), using the beam-hardening correction of 26 % and the ring-artefact correction of 6. No smoothing was applied. All µCT images were analyzed qualitatively using CTVox (v.3.3.1.0, Bruker, Belgium). Severity grading of tibiae included "normal" for tibiae with < 3 clear-rimmed lesions and "pathologic" for tibiae with ≥ 3 clear-rimmed lesions. Of note, some tibiae demonstrated small (likely age-related) spots of qualitatively lower bone density, which appeared different from the defined lesions and were excluded from the severity grading. Skull images were graded as "normal" as long as areas of qualitatively lower bone density were absent or only locally restricted and "pathologic" once these areas were diffuse and/or accompanied with lesions.

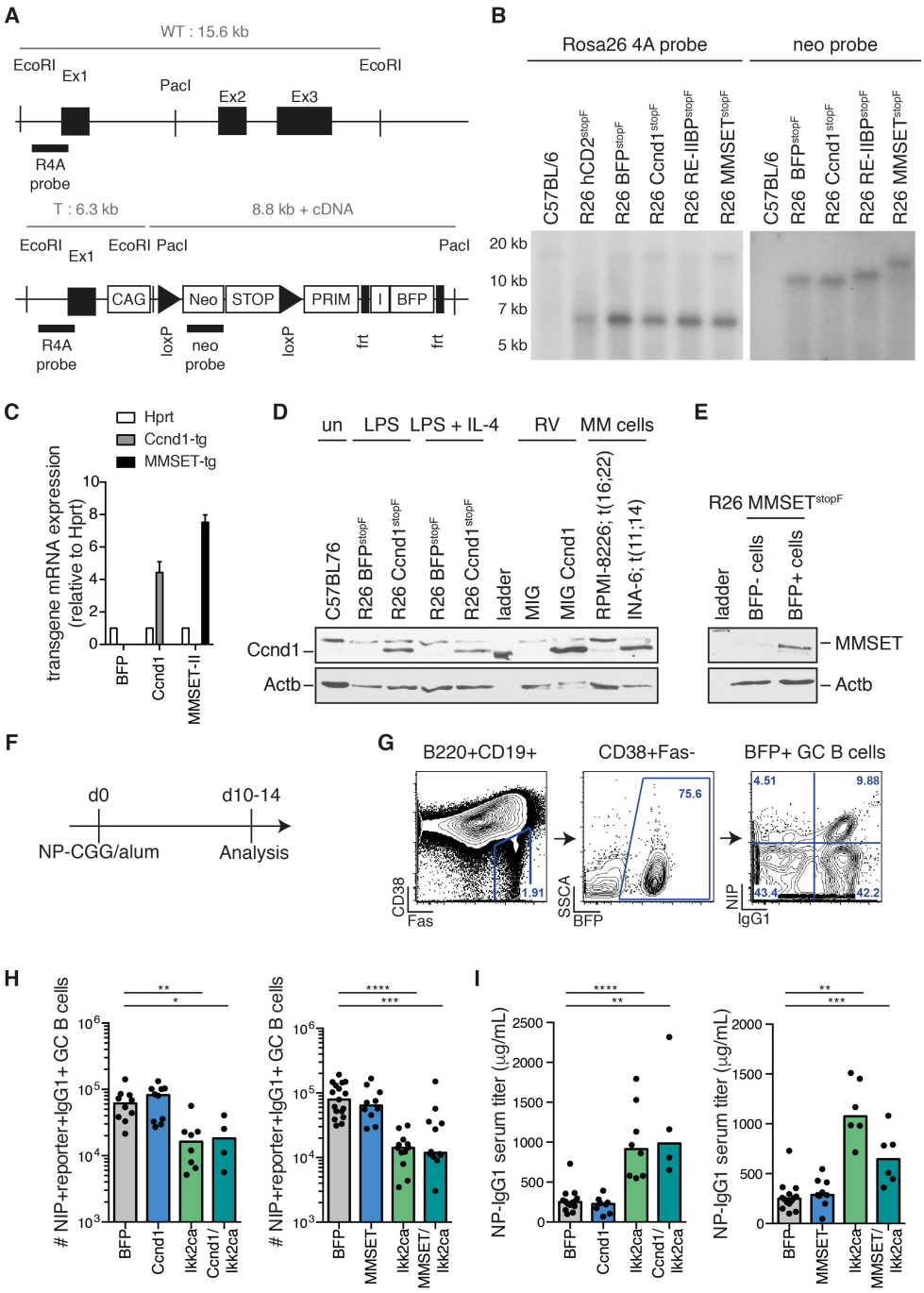

Fig. S1. Gene targeting strategy, validation of expression and functional analysis of the newly generated conditional alleles for Ccnd1 and MMSET. (**A**) Scheme of the wildtype (WT) and targeted (T) Rosa26 locus. Ex = exon; CAG = CAG promoter; Neo = Neomycin resistance gene; STOP = STOP cassette; PRIM = primary candidate, i.e., Ccnd1 or MMSET; I = IRES (internal ribosomal entry site); BFP = blue fluorescent protein; R4A and neo denote Southern blot probes. (**B**) Southern blot for Rosa26 4A (R4A) and neo probes on EcoRI- or PacI-digested tail genomic DNA of the indicated mouse genotypes. Note: The MMSET isoform RE-IIBP was also targeted but not used in this study. (**C-D**) Splenic B cells were isolated, treated with TATCre recombinase and cultured with LPS or LPS and IL-4. 48 h later BFP+ cells were sorted and subjected to RNA and protein analysis. (C) Quantitative PCR using primers to detect transgenic

Ccnd1 (Ccnd1-tg), transgenic *MMSET* (MMSET-tg) and *Hprt* (control) mRNA expression, respectively. (D) Immunoblot for Ccnd1 on whole cell lysates of transgenic B cells, C57BL/6 B cells retrovirally transduced with empty vector (MIG) or MIG-Ccnd1 as well as human MM cell lines. (**E**) To detect MMSET protein expression, splenic B cells were isolated, treated with TATCre recombinase and differentiated into plasma cells using the 40LB feeder cell system (3). After 8 days (4d IL-4; 2x 2d IL-21) BFP+ and BFP- B220lowCD138+ plasma cells were sorted and analyzed for MMSET expression by Western blot. Actb (ß-actin) served as loading control. (**F-I**) Analysis of the immune response to NP-CGG. (F) Immunization scheme. Control (BFP), single mutant (Ccnd1 or MMSET or Ikk2ca) and double mutant (Ccnd1/Ikk2ca or MMSET/Ikk2ca) mice were immunized once with NP-CGG and analyzed at day 10-14. (G) Gating strategy for antigen (NIP)-specific GC B cells (pre-gate: B220+CD19+ B cells). (H) Absolute numbers of splenic NIP-specific IgG1+ GC B cells; each dot represents one mouse. (I) NP-specific IgG1 serum titers measured by ELISA. Statistics: Mann-Whitney-test; *p<0.05; **p<0.01; ***p<0.001; ****p<0.0001.

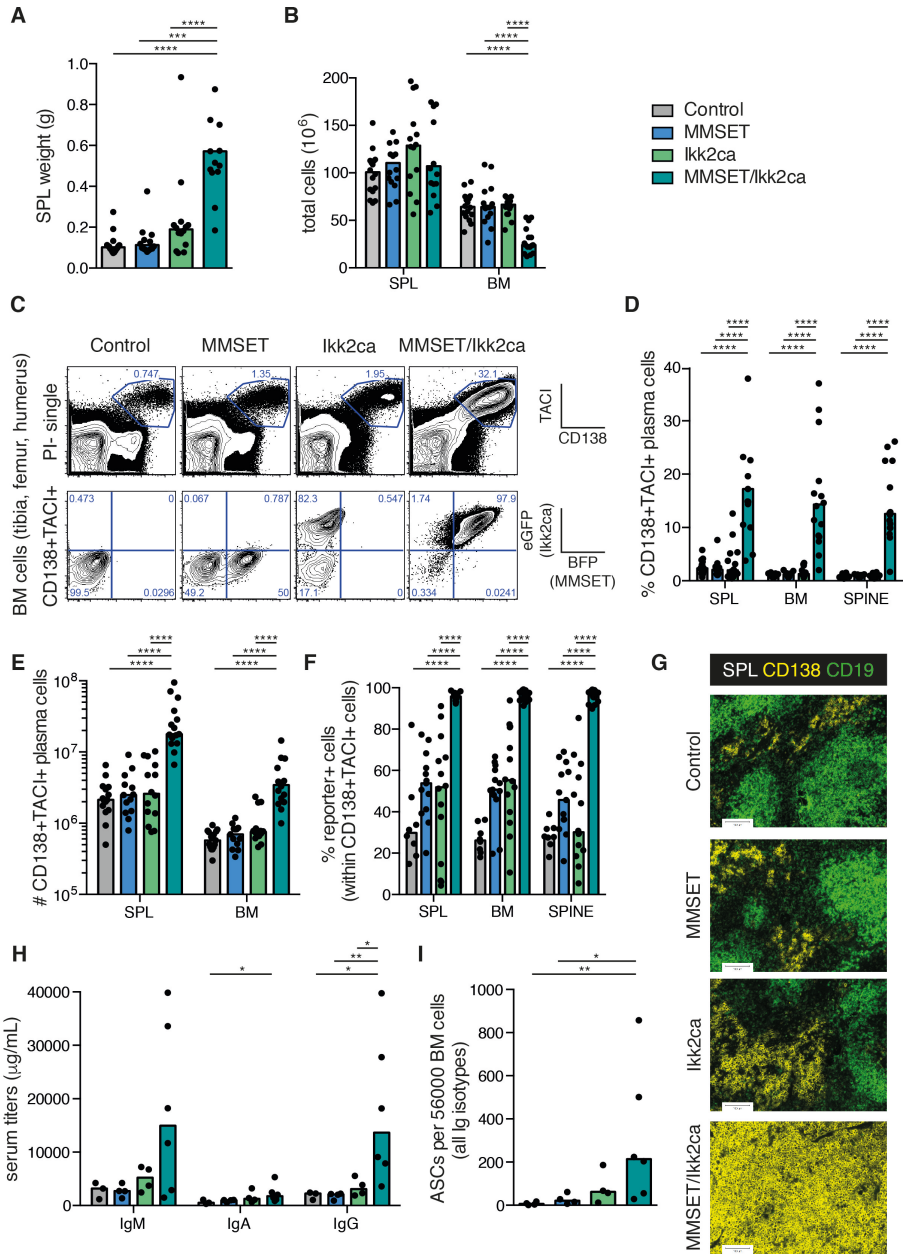

Fig. S2. Characterization of the plasma cell expansion in aged MMSET/Ikk2ca mice. (**A**) Spleen weight and (**B**) total cell numbers of the spleen and BM (isolated from one tibia, one femur and one humerus) of mice with the indicated genotypes. (**C**) Representative flow cytometry contour plots of BM isolated from mice with the indicated genotypes depicting CD138+TACI+ plasma cells (upper panel) and reporter expression within this population (lower panel). (**D**) Percentage of CD138+TACI+ plasma cells within the spleen, long bone-derived BM and spine-derived BM. (**E**) Absolute numbers of CD138+TACI+ plasma cells within the spleen and long bone-derived BM. (**F**) Reporter (BFP and/or GFP) expression within CD138+TACI+ plasma cells of the spleen, long bone-derived BM and spine-derived BM. (**G**) Representative immunofluorescence images of spleen sections stained with α-CD19 (green, B cells) and α-CD138 (yellow, plasma cells). (**H**) ELISA of total serum IgM, IgG and IgA titers. (**I**) ELISPOT analysis of immunoglobulin isotypes (combination of α-IgM, α-IgG1, α-IgG2a/b/c, α-IgG3, α-IgA) on thawed long bone-derived total BM cells. Statistics: Mann-Whitney-test; *p<0.05; **p<0.01; ***p<0.001; ****p<0.0001.

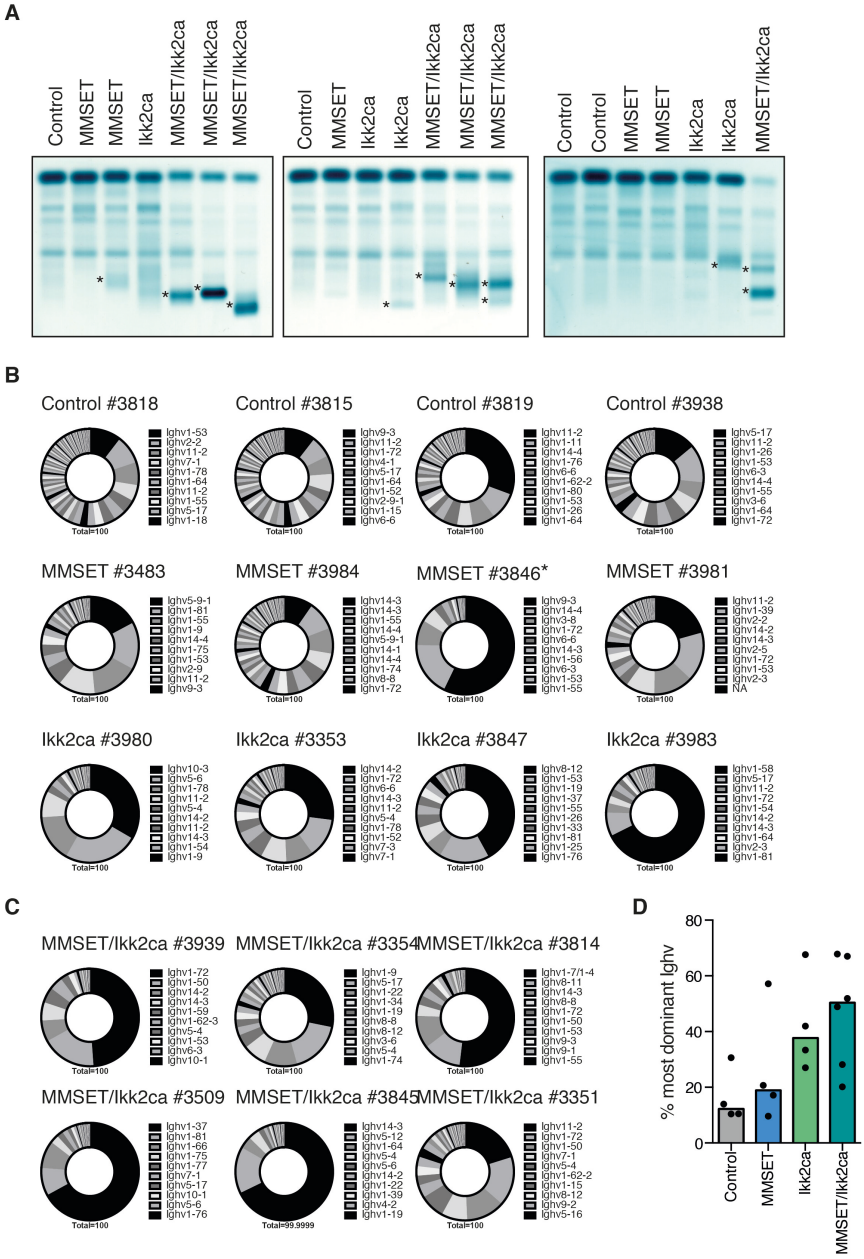

Fig. S3. MMSET/Ikk2ca plasma cells show a clonally restricted Ighv gene repertoire (extension to Fig. 1G). (**A**) Representative serum protein electrophoresis (SPEP) of more MMSET cohort mice; M spikes are marked with an asterisk. (**B-D**) 2,000 long bone-derived transgenic (reporter+) CD138+TACI+ BM plasma cells of aged cohort mice were sorted and analyzed by RNA-Seq. (B-C) Pie charts depict the fraction of individual Ighv genes among all annotated Ighv gene reads for cohort mice of the indicated genotypes. Shown are the results for all animals of the entire cohort analyzed by RNA-seq; i.e., control and single mutant (B) and double mutant (C) mice. The 10 most dominantly expressed Ighv genes are listed. Pie charts need to be read clockwise. Note: only 1,000 plasma cells could be sorted from MMSET mouse #3846. (D) Graph illustrating the fraction of the most dominant Ighv gene per mouse of the indicated genotypes.

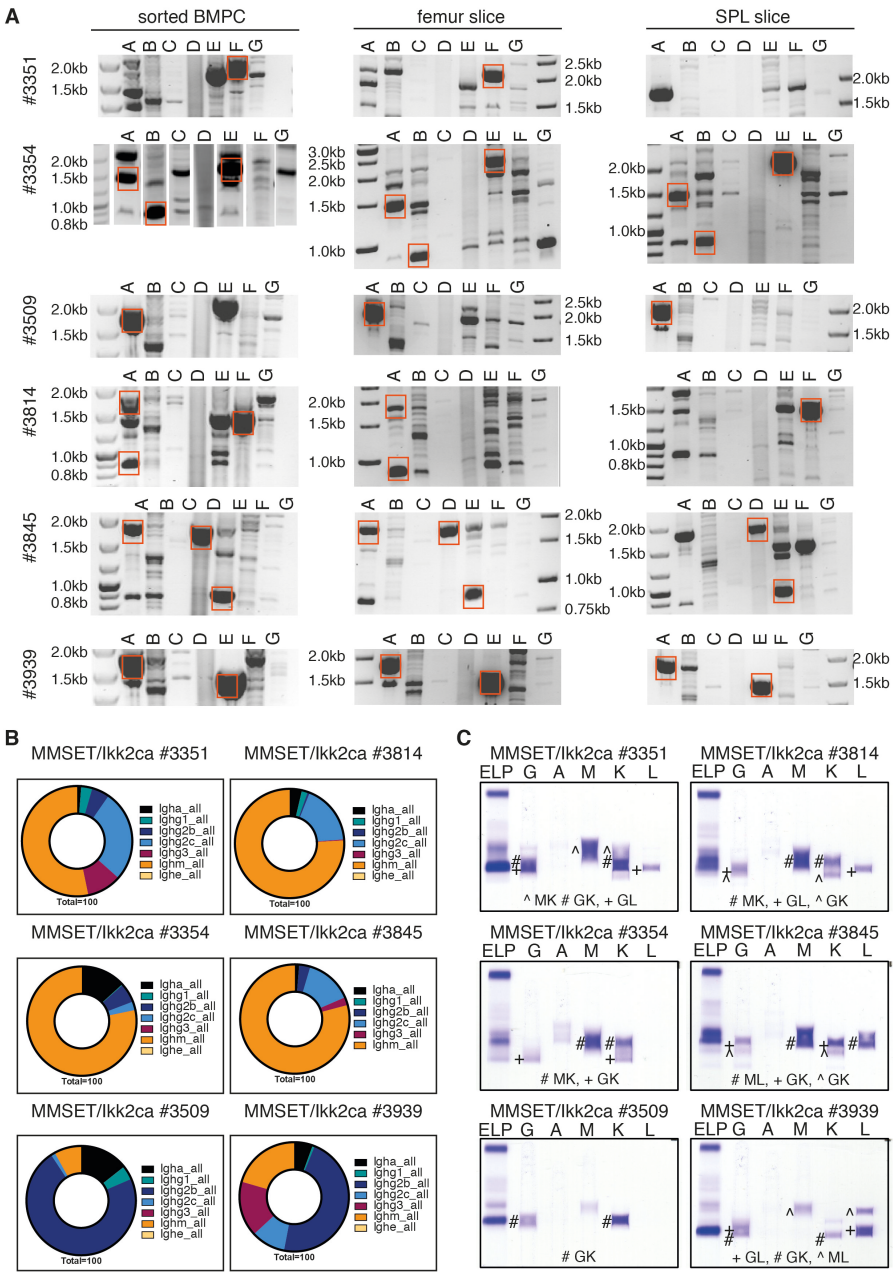

Fig. S4. The sorted MMSET/Ikk2ca plasma cells reflect the actual clonal composition. (**A**) Genomic DNA was isolated from sorted reporter+ CD138+TACI+ BM plasma cells (left panel), a femur slice (middle panel) or a spleen slice (right panel) and subjected to VDJ-PCR analysis covering the Ighv gene families J558 (VHA), Q52 (VHB), 36-60 (VHC), X24 (VHD), 7183 (VHE), J606 and S107 (VHF) and GAM3 (VHG) (5). Orange boxes mark shared clones between sorted cells and either femur or spleen sections. The respective VDJ rearrangements and CDR3 sequences are summarized in Table S2. (**B**) Pie charts depict the fraction of individual Igh isotypes among all annotated Igh isotype gene reads determined by RNA-Seq of sorted BFP+GFP+ CD138+TACI+ MMSET/Ikk2ca BM plasma cells. (**C**) SPEP coupled to immunofixation of the six MMSET/Ikk2ca mice whose BM plasma cells were also used for RNA-sequencing showing the Ig heavy and light chain isotypes of the detected M proteins. Corresponding Ig light and heavy chains are marked with the same symbol; abbreviations: A - IgA, M - IgM, G - IgG, K - Igκ, L - Igλ.

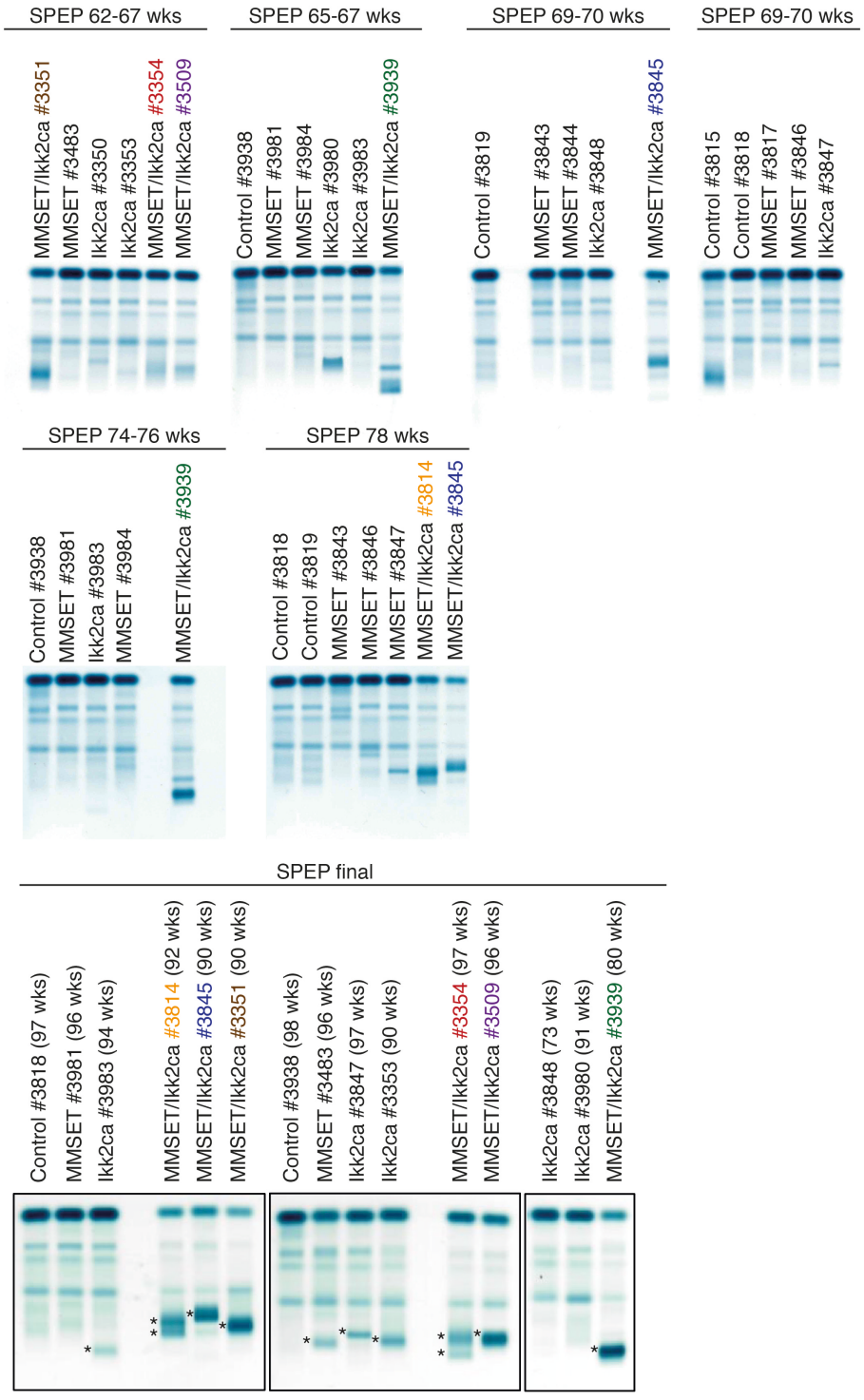

Fig. S5. Longitudinal serum protein electrophoresis of MMSET/Ikk2ca cohort mice. MMSET/Ikk2ca cohort mice were bled at the indicated weeks of age and the serum was analyzed by electrophoresis. Individual MMSET/Ikk2ca mice are color-coded. Shown are two or three analysis time points per mouse.

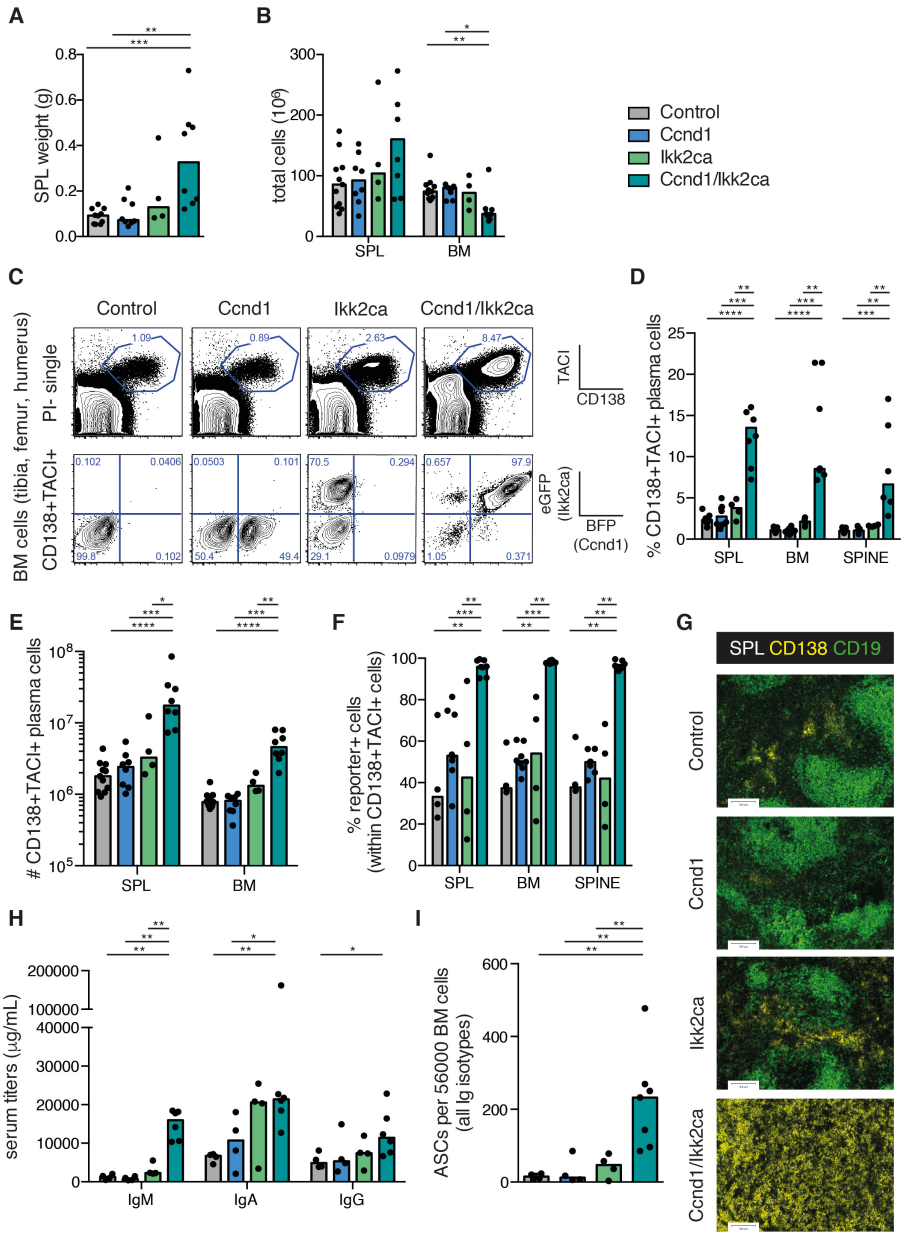

Fig. S6. Characterization of the plasma cell expansion in aged Ccnd1/Ikk2ca mice. (**A**) Spleen weight and (**B**) total cell numbers of the spleen and BM (isolated from one tibia, one femur and one humerus) of mice with the indicated genotypes. (**C**) Representative contour plots of the long bone-derived BM depicting CD138+TACI+ plasma cells (upper panel) and reporter expression within this population (lower panel). (**D**) Percentage of CD138+TACI+ plasma cells within the spleen, long bone-derived BM and spine-derived BM. (**E**) Absolute numbers of CD138+TACI+ plasma cells within the spleen and long bone-derived BM. (**F**) Relative reporter (BFP and/or GFP) expression within CD138+TACI+ plasma cells of the spleen, long bone-derived BM and spine-derived BM. (**G**) Representative immunofluorescence images of spleen sections stained with α-CD19 (green, B cells) and α-CD138 (yellow, plasma cells). (**H**) ELISA of total serum IgM, IgG and IgA titers. (**I**) ELISPOT analysis of immunoglobulin isotypes (combination of α-IgM, α-IgG1, α-IgG2a/b/c, α-IgG3, α-IgA) on thawed total BM cells. Statistics: Mann-Whitney-test; *p<0.05; **p<0.01; ***p<0.001; ****p<0.0001.

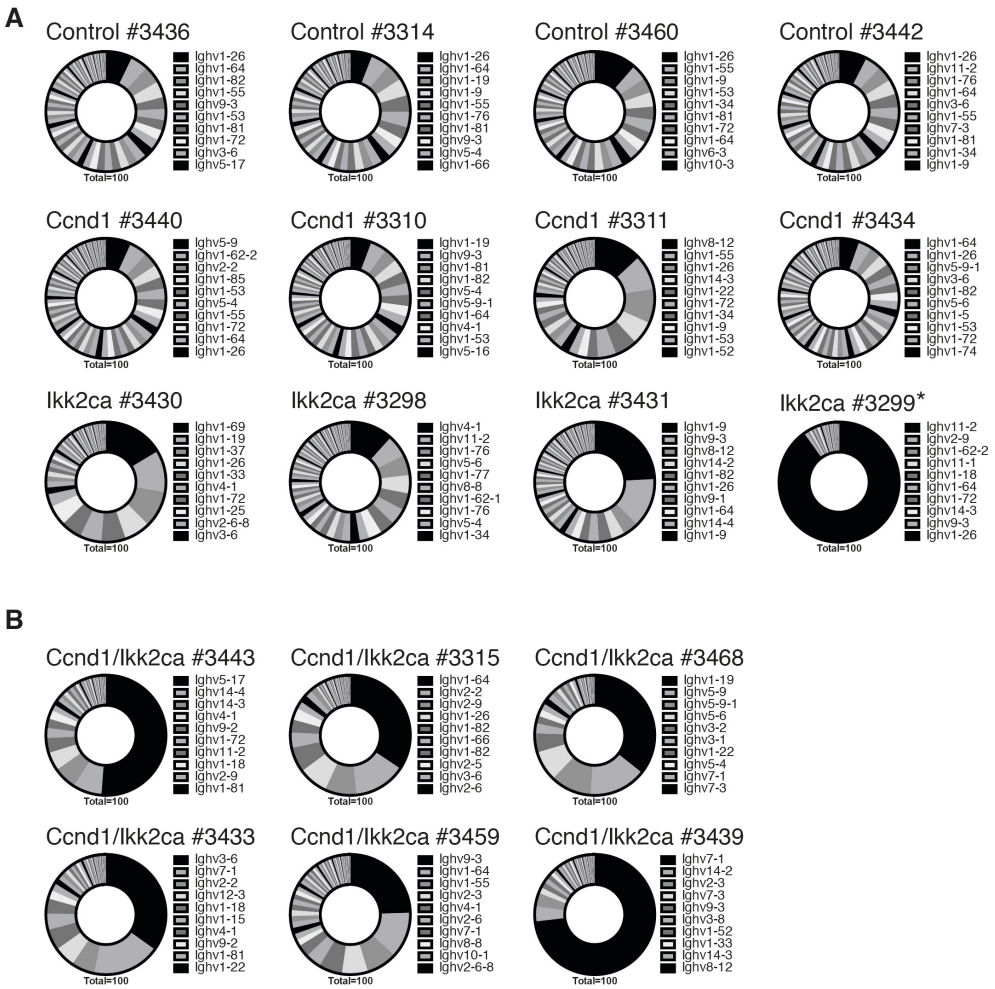

Fig. S7. Ccnd1/Ikk2ca plasma cells are clonally restricted (extension to Fig. 3D). 2,000 long bone-derived transgenic (reporter+) CD138+TACI+ BM plasma cells of aged cohort mice were sorted and analyzed by RNA-Seq. Pie charts depict the fraction of individual Ighv genes among all annotated Ighv gene reads for cohort mice of the indicated genotypes. Shown are the results for all animals of the entire cohort analyzed by RNA-seq; control and single mutant mice (**A**) and double mutant mice (**B**). The 10 most dominantly expressed Ighv genes are listed. Pie charts need to be read clockwise. Note: Ikk2ca mouse #3299 presented with a monoclonal B cell tumor.

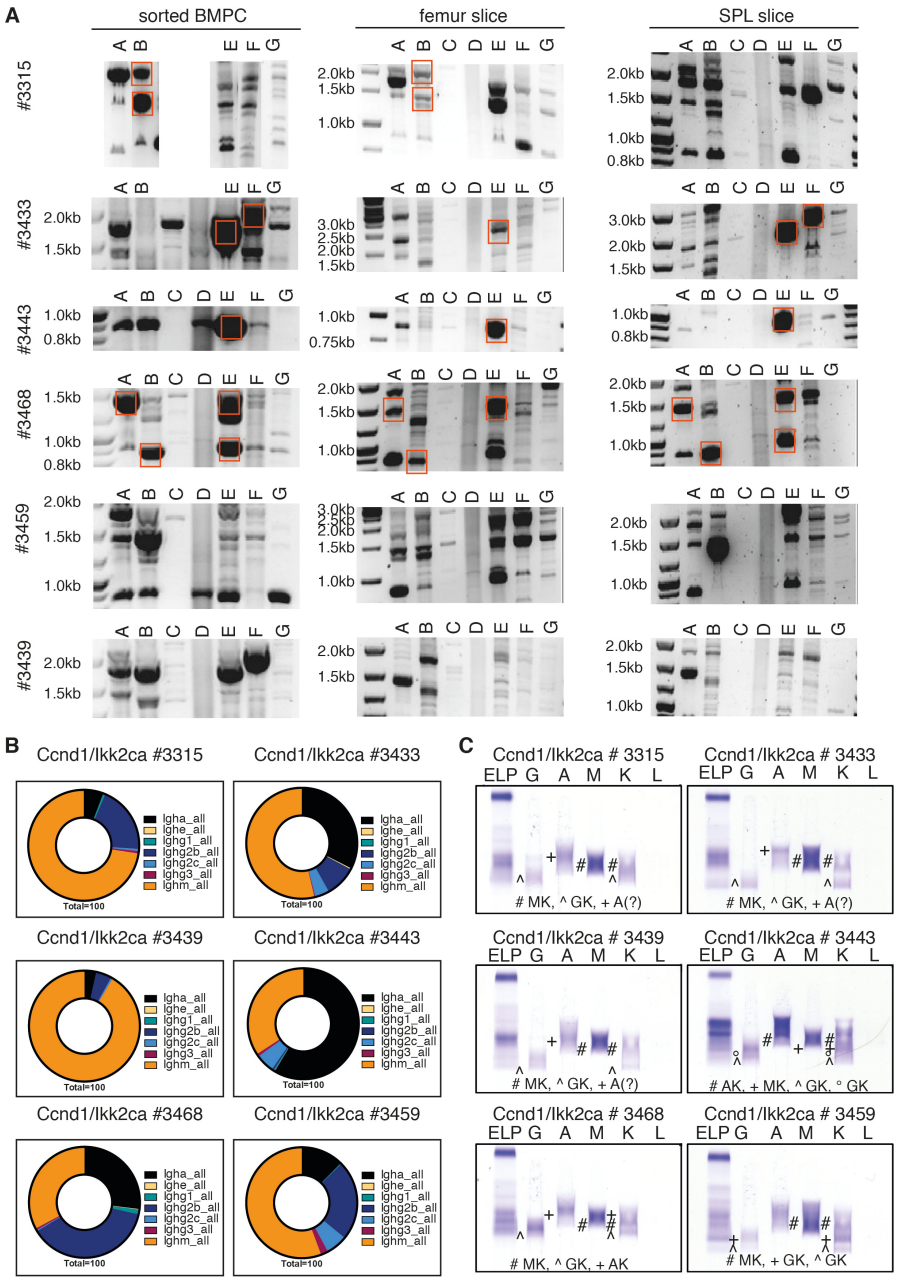

Fig. S8. The sorted Ccnd1/Ikk2ca plasma cells reflect the actual clonal composition. (**A**) Genomic DNA was isolated from sorted reporter+ CD138+TACI+ BM plasma cells (left panel), a femur slice (middle panel) or a spleen slice (right panel) and subjected to VDJ-PCR analysis covering the Ighv gene families J558 (VHA), Q52 (VHB), 36-60 (VHC), X24 (VHD), 7183 (VHE), J606 and S107 (VHF) and GAM3 (VHG) (5). Orange boxes mark shared clones between sorted cells and either femur or spleen sections. The respective VDJ rearrangements and CDR3 sequences are summarized in Table S4. (**B**) Pie charts depict the fraction of individual Igh isotypes among all annotated Igh isotype gene reads determined by RNA-Seq of sorted BFP+GFP+ CD138+TACI+ Ccnd1/Ikk2ca BM plasma cells. (**C**) SPEP coupled to immunofixation of the six Ccnd1/Ikk2ca mice whose BM plasma cells were also used for RNA-sequencing showing the Ig heavy and light chain isotypes of the detected M proteins. Corresponding Ig light and heavy chains are marked with the same symbol; abbreviations: A - IgA, M - IgM, G - IgG, K - Igκ, L - Igλ.

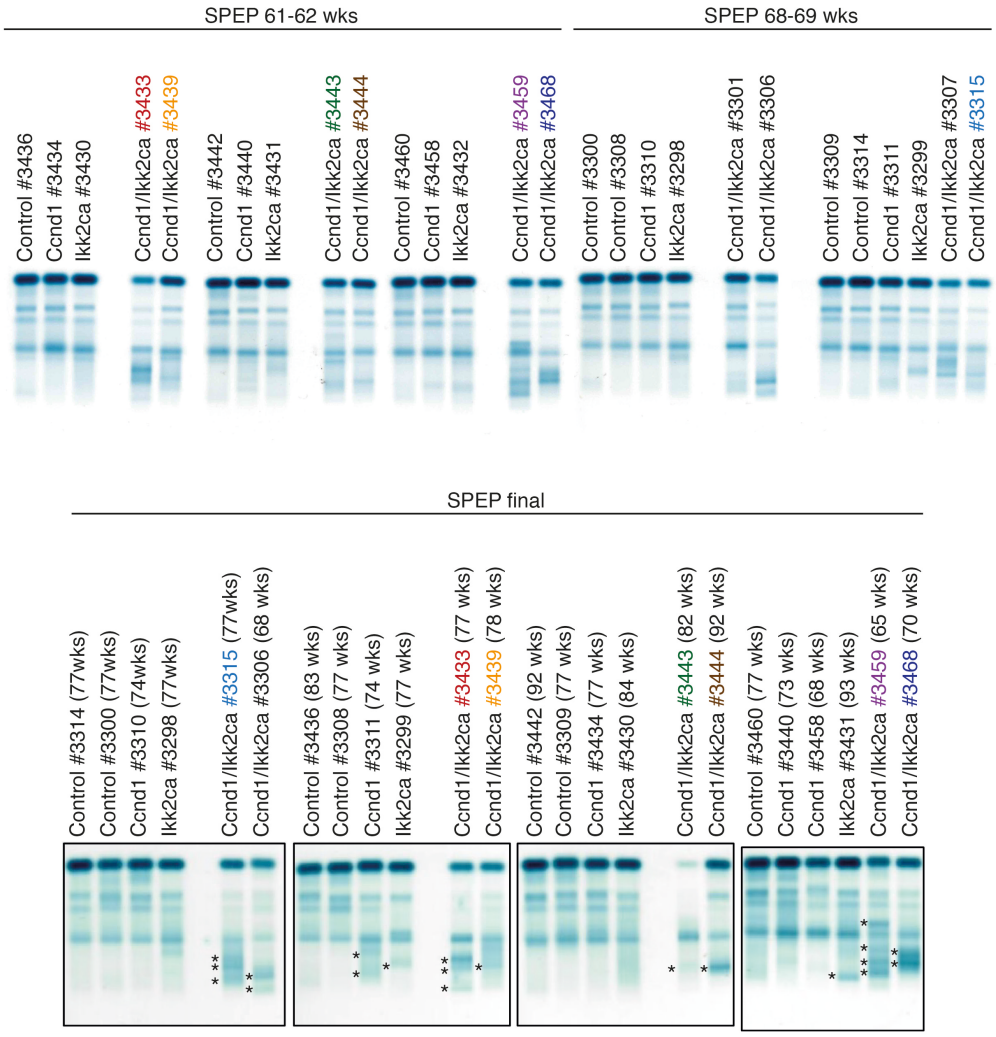

Fig. S9. Longitudinal serum protein electrophoresis of Ccnd1/Ikk2ca cohort mice. Ccnd1/Ikk2ca cohort mice were bled at the indicated weeks of age and the serum was analyzed by electrophoresis. Individual Ccnd1/Ikk2ca mice are color-coded. Shown are two analysis time points per mouse.

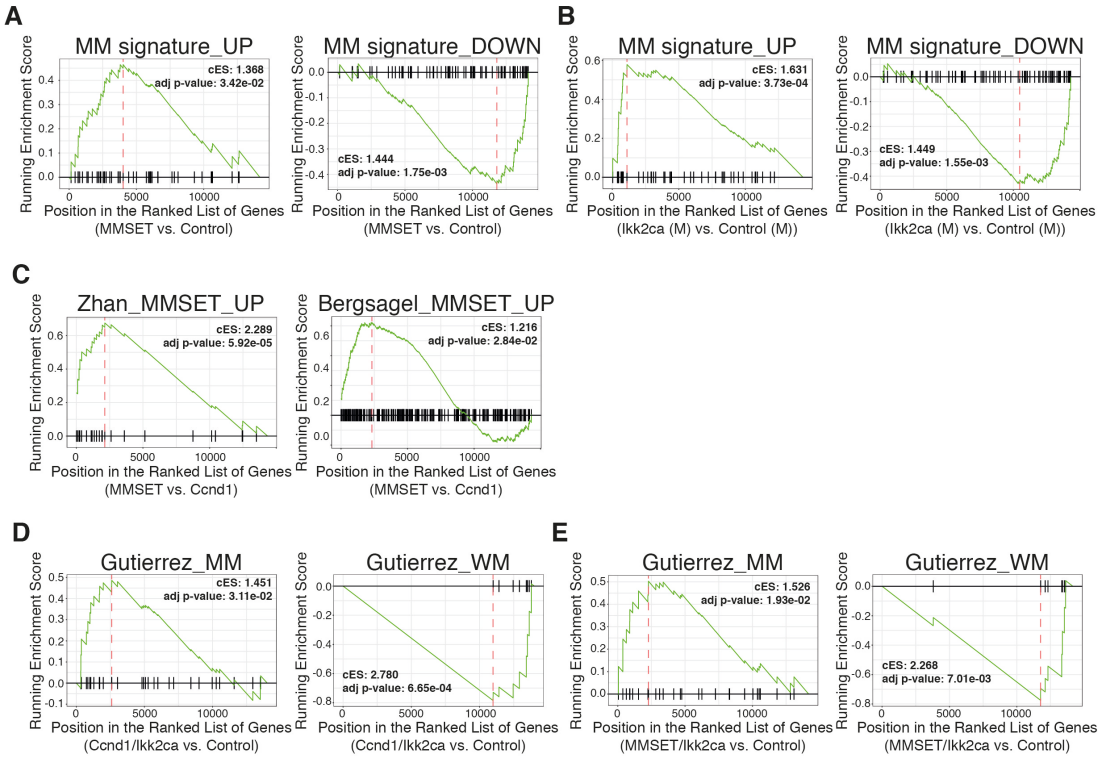

Fig. S10. GSEA analyses of human MM and Waldenström's Macroglobulinemia (WM) signature genes in transgenic mouse plasma cells (extension to Fig. 5). Graphical representation of gene set enrichment analyses employing the tmod algorithm (18). (**A-B**) The x-axis shows the ranked gene list (ordered from most up- to most down-regulated) when comparing MMSET (A) or Ikk2ca (B) to control mouse BM plasma cells. The tested gene sets include genes differentially up- (MM signature_UP) or down-regulated (MM signature_DOWN) in human MGUS/MM cells versus normal human plasma cells (11),(12). (**C**) The x-axis shows the ranked gene list (ordered from most up- to most down-regulated) when comparing MMSET and Ccnd1 BM plasma cells. The tested gene sets includes genes specifically up-regulated in the t(4;14)/MMSET subgroup of MM patients (14),(15). (**D-E**) The x-axis shows the ranked gene list (ordered from most up- to most down-regulated) when comparing Ccnd1/Ikk2ca (D) or MMSET/Ikk2ca (E) to control mouse BM plasma cells. The tested gene sets include genes specifically up-regulated in human MM (Gutierrez_MM) or human WM (Gutierrez_WM) cells versus normal human plasma cells (13).

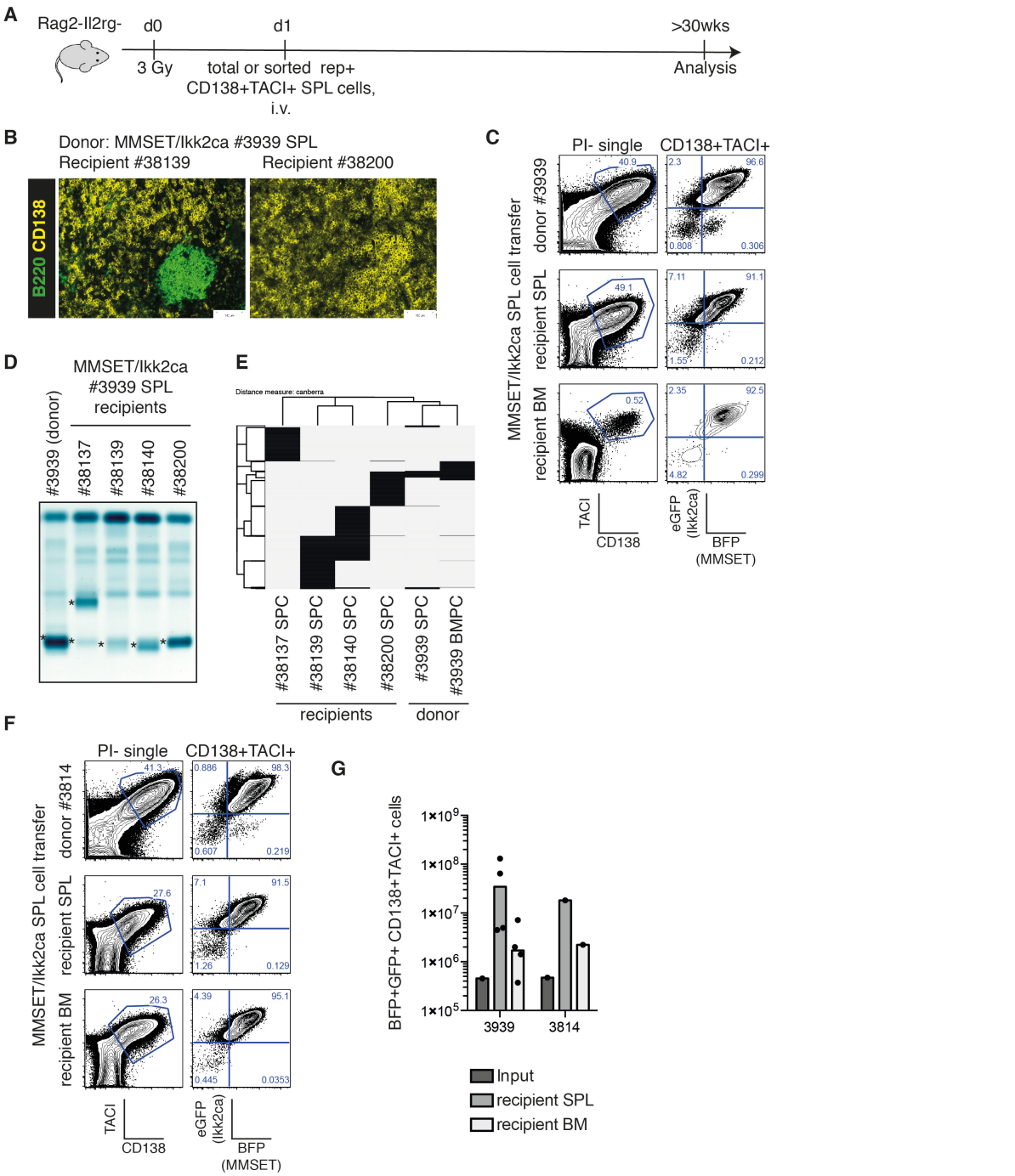

Fig. S11. Continued analysis of MMSET/Ikk2ca spleen cell recipient mice (extension to Fig. 6). (**A**) Experimental scheme showing the transfer of double mutant splenocytes into sublethally irradiated (3 Gy) Rag2-Il2r- immunodeficient recipients. (**B**) Immunofluorescence images of the other two MMSET/Ikk2ca #3939 recipient spleens stained with α-B220 (green, B cells) and α-CD138 (yellow, plasma cells). (**C**) Representative contour plots depicting CD138+TACI+ plasma cells and the reporter expression within this population for the MMSET/Ikk2ca donor #3939. Upper panel: MMSET/Ikk2ca donor spleen; lower panel: representative recipient spleen and long bone-derived BM. (**D**) SPEP of the MMSET/Ikk2ca donor #3939 and its corresponding four recipients; M spikes are marked (*). (**E**) Double mutant (BFP+GFP+) plasma cells were sorted from all four MMSET/Ikk2ca #3939 recipients' spleens

(SPC) as well as the donor #3939 spleen (SPC) and bone marrow (BMPC) and subjected to WES to determine additionally acquired somatic mutations (reference: #3939 BM myeloid cells). The graph depicts shared mutations (black lines) between the recipients and donor plasma cells. (**F**) Representative contour plots depicting CD138+TACI+ plasma cells and the reporter expression within this population for a second MMSET/Ikk2ca donor #3814. Upper panel: MMSET/Ikk2ca donor spleen; lower panel: representative recipient spleen and long bone-derived BM. (**G**) Shown are absolute numbers of CD138+TACI+ plasma cells in the spleen and long bone-derived BM of recipient mice as well as the input cell number of donor plasma cells for the two MMSET/Ikk2ca donors #3939 and #3814.

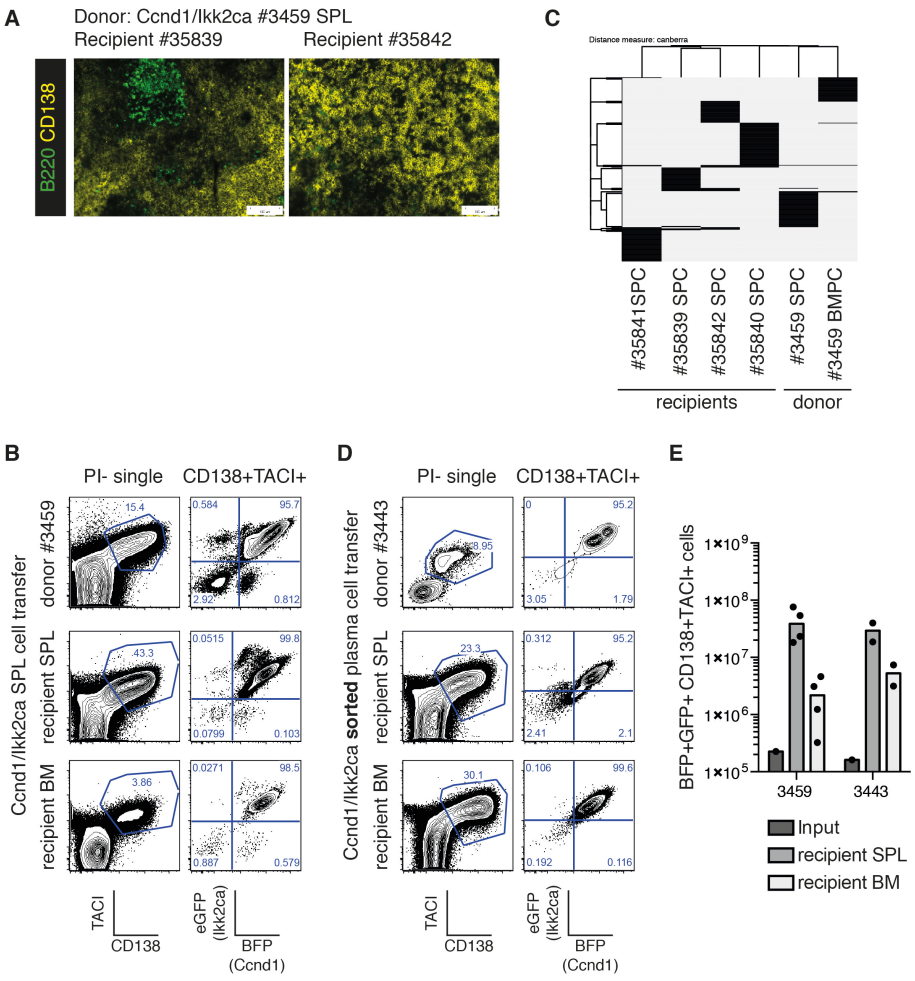

Fig. S12. Continued analysis of Ccnd1/Ikk2ca spleen cell recipient mice (extension to Fig. 6). (**A**) Immunofluorescence images of the other two Ccnd1/Ikk2ca #3459 recipient spleens stained with α-B220 (green, B cells) and α-CD138 (yellow, plasma cells). (**B**) Representative contour plots depicting CD138+TACI+ plasma cells and the reporter expression within this population for the Ccnd1/Ikk2ca donor #3459. Upper panel: Ccnd1/Ikk2ca donor spleen; lower panel: representative recipient spleen and long bone-derived BM. (**C**) Double mutant (BFP+GFP+) plasma cells were sorted from all four Ccnd1/Ikk2ca #3459 recipients' spleens (SPC) as well as the donor #3459 spleen (SPC) and bone marrow (BMPC) and subjected to WES to determine additionally acquired somatic mutations (reference: #3459 BM myeloid cells). The graph depicts shared mutations (black lines) between the recipients and donor plasma cells. (**D**) An optimized transfer strategy was applied for a second Ccnd1/Ikk2ca donor (#3443) based on the transplantation of approx. 1.6 x 10^5 sorted BFP+GFP+ CD138+TACI+ and CD19- splenic plasma cells along with 1 x 10^6 Rag2-Il2r- carrier spleen cells into irradiated (3 Gy) Rag2-Il2r- recipient mice. Representative contour plots depicting CD138+TACI+ plasma cells and the reporter expression within this population. Upper panel: sorted Ccnd1/Ikk2ca #3443 donor splenic plasma cells; lower panel: representative recipient spleen and long bone-derived BM. (**E**) Shown are absolute numbers of CD138+TACI+ plasma cells in the spleen and long bone-derived BM of recipient mice as well as the input cell number of donor plasma cells for the two Ccnd1/Ikk2ca donors #3459 and #3443.

Tab. S1. Histopathologic evaluation of femur and spleen sections from MMSET cohort mice. Sections from spleens and femurs of aged control, single (MMSET, Ikk2ca) and double mutant (MMSET/Ikk2ca) mice were stained with HE and evaluated in a blinded fashion without knowledge of the underlying genotype. ND, denotes not determined.

ID	genotype	Femur	Spleen
3815	Control	ND	enrichment of plasma cells
3818	Control	normal	plasma cell hyperplasia in marginal zone
3819	Control	normal	plasma cell hyperplasia in marginal zone
3938	Control	normal	plasma cell hyperplasia in marginal zone
5230	Control	normal	ND
4978	Control	normal	ND
4977	Control	normal	ND
3483	MMSET	normal	plasma cell hyperplasia in marginal zone
3846	MMSET	diffuse myeloma infiltrate (99 %)	tumor-forming plasma cell infiltrates, destruction of architecture
3981	MMSET	normal	plasma cell hyperplasia in marginal zone
3984	MMSET	normal	plasma cell hyperplasia in marginal zone
5250	MMSET	normal	ND
5253	MMSET	normal	ND
4979	MMSET	normal	ND
3353	Ikk2ca	diffuse myeloma infiltrate (70 %)	tumor-forming plasma cell infiltrates, destruction of architecture
3847	Ikk2ca	focal myeloma infiltrate (approx. 5 %)	tumor-forming plasma cell infiltrates, destruction of architecture
3980	Ikk2ca	normal	nodular plasma cell infiltrates
3983	Ikk2ca	normal	plasma cell hyperplasia in marginal zone
5250	Ikk2ca	normal	ND
5643	Ikk2ca	normal	ND
5161	Ikk2ca	normal	ND
5261	Ikk2ca	normal	ND
3351	MMSET/ Ikk2ca	diffuse myeloma infiltrate (90 %)	tumor-forming plasma cell infiltrates, destruction of architecture
3354	MMSET/ Ikk2ca	diffuse myeloma infiltrate (approx. 80 %)	tumor-forming plasma cell infiltrates, destruction of architecture
3509	MMSET/ Ikk2ca	diffuse myeloma infiltrate (90 %)	tumor-forming plasma cell infiltrates, destruction of architecture
3814	MMSET/ Ikk2ca	diffuse myeloma infiltrate (99 %)	tumor-forming plasma cell infiltrates, destruction of architecture
3845	MMSET/ Ikk2ca	diffuse myeloma infiltrate (90 %)	tumor-forming plasma cell infiltrates, destruction of architecture
3939	MMSET/ Ikk2ca	diffuse myeloma infiltrate (99 %)	tumor-forming plasma cell infiltrates, destruction of architecture
5409	MMSET/ Ikk2ca	diffuse myeloma infiltrate (40 %)***	ND
5160	MMSET/ Ikk2ca	diffuse myeloma infiltrate (80 %)	ND
5258	MMSET/ Ikk2ca	normal	ND
5408	MMSET/ Ikk2ca	focal myeloma infiltrate (10%)*	ND
4997	MMSET/ Ikk2ca	focal myeloma infiltrate (20%)**	ND

5434	MMSET/ Ikk2ca	diffuse myeloma infiltrate (50 %)****	ND
4995	MMSET/ Ikk2ca	diffuse myeloma infiltrate (90 %)	ND
5075	MMSET/ Ikk2ca	diffuse myeloma infiltrate (80 %)	ND
5259	MMSET/ Ikk2ca	diffuse myeloma infiltrate (90 %)	ND

NOTE: Most MMSET/Ikk2ca mice that did not show ≥ 60% myeloma infiltration in the femur biopsy still presented with MM-associated clinical features reaching a myeloma-defining event (IMWG criteria (29)).

*5408: increased calcium (9.93 mg/dL), low albumin (22.36 g/L), low RBCs (6.74 M/µL), low platelets (49 K/µL), tibia lesions
**4997: increased calcium (9.73 mg/dL), low hemoglobin (6.80 g/dL), low albumin (20.35 g/L), low RBCs (4.05 M/µL), low platelets (93 K/µL)
***5409: increased calcium (9.67 mg/dL), low hemoglobin (7.9 g/dL), low albumin (15.22 g/L), low RBCs (5.56 M/µL), low platelets (384 K/µL)
****5434: low hemoglobin (8.00 g/dL), low albumin (13.25 g/L), low RBCs (4.87 M/µL), low platelets (231 K/µL), tibia lesions, skull osteopenia

Tab. S2. Overview of dominant VDJ rearrangements of MMSET/Ikk2ca plasma cells determined by VDJ-PCR. Abbreviations: P/NP = productive/non-productive rearrangement; tissue = SPL (spleen section), F (femur section), BMPC (sorted BM plasma cells); #SHM = amount of somatic hypermutation within VDJ rearrangement.

ID	genotype	PCR fragment	VDJ rearrangement	CDR3	P/NP	tissue	# SHM
3354	MMSET/ Ikk2ca	VHE-JH1	Ighv5-17*01; Ighd1-1*01; Ighj1*03	GCAAGGCCCTTTACTACGATAGGA GCTACGTACTGGTACTTCGATGTC	P	SPL, F, BMPC	0
		VHB-JH4	Ighv2-6-5*01; Ighd2-1*01; Ighj4*01	GCCAAATACTATGGTAACTACTATG CTATGGACTAC	P	SPL, F, BMPC	5 to 8
		VHA-JH3	Ighv1-37*01; Ighd2-1*01; Ighj3*01	GCAAGATTTCTCAGTCTACTATGGT AACGGTGGGCCTGGTTTGCTTAC	NP	SPL, F, BMPC	0
3814	MMSET/ Ikk2ca	VHF-JH3	Ighv6-6*01; Ighd2-1*01; Ighj3*01	ACCAGGCCGGGCTATGGTAACCCC TGGTTTGCTTAC	P	SPL, BMPC	1 to 3
		VHA-JH2	Ighv1-4*01/Ighv1-7*01; Ighd1-1*01; Ighj2*01	GCAACCCCTTATTACTACGGTAGTA GCTACAACTAC	P	SPL, F, BMPC	5 to 8
		VHA-JH4	Ighv1-81*01/Ighd1-2*01/Ighj4*01	GCAAGAGGTATTACTACGGCTACTA CTATGCTATGGACTAC	NP	F, BMPC	13 to 15
3845	MMSET/ Ikk2ca	VHE-JH4	Ighv5-12*01; Ighd2-4*01; Ighj4*01	GCAAGACATGATTACGAGGGGCCT AACTATGCTATGGACTAC	P	SPL, F, BMPC	0 to 1
		VHA-JH2	Ighv1s135*01/Ighd2-14*01/Ighj2*01	GCAAGAGAGGGGGAAAACTTGAGG TACGACGAGGGAGGGGTTGACTAC	P	F, BMPC	1 to 2
		VHD-JH1	Ighv4-2*01; N/A; Ighj2*01	GCAAGACAGGGGTACTACTTTGAC TAC	NP	SPL, F, BMPC	0 to 2
		Ighv14-3-JH4	Ighv14-3*02; Ighd2-14*01; Ighj4*01	GCTAGATACTATAGGTACCTCTATG CTATGGACTAC	P	F	0
3939	MMSET/ Ikk2ca	VHE-JH3	Ighv5-4*02; Ighd2-14*01; Ighj3*01	GCAAGAGATCGGTTCCCAATAGGT ACGACGTTTTGCTTAC	NP	SPL, F, BMPC	0 to 1
		VHA-JH2	Ighv1-72*01; Ighd3-2*02; Ighj2*01	GCAAGAGGACAGCTCAGGCTTCAC TTTGACTAC	P	SPL, F, BMPC	0
3509	MMSET/ Ikk2ca	VHA-JH2	Ighv1-37*01; Ighd2-4*01; Ighj2*01	GCAAGAGGGGGGAGCTATGATTAC GACAGGATGTACTTTGACTAC	P	SPL, BMPC	0 to 2
3351	MMSET/ Ikk2ca	VHF-JH1	Ighv11-2*02; Ighd2-1*01; Ighj1*01	ATGAGATATGGTAACTACTGGTACT TCGATGTC	P	F, BMPC	0
		VHA-JH1	Ighv1-72*01; Ighd2-3*01; Ighj2*01	GCTCGCTATGATGGTTACCTTTTTG ACTAC	P	SPL	0

Tab. S3. Histopathologic evaluation of femur and spleen sections from Ccnd1 cohort mice. Sections from spleens and femurs of aged control, single (Ccnd1, Ikk2ca) and double mutant (Ccnd1/Ikk2ca) mice were stained with HE and evaluated in a blinded fashion without knowledge of the underlying genotype.

ID	genotype	Femur	Spleen
3314	Control	normal	normal
3436	Control	normal	normal
3442	Control	normal	normal
3460	Control	normal	normal
3310	Ccnd1	normal	normal
3311	Ccnd1	normal	normal
3434	Ccnd1	normal	normal
3440	Ccnd1	normal	normal
3298	Ikk2ca	normal	normal
3299	Ikk2ca	normal	normal
3430	Ikk2ca	normal	myeloma infiltrate
3431	Ikk2ca	normal	normal
3315	Ccnd1/ Ikk2ca	myeloma infiltrate (80 %)	extensive myeloma infiltrate in red pulp
3433	Ccnd1/ Ikk2ca	myeloma infiltrate (80 %), signs of bone remodeling	extensive myeloma infiltrate w/ destruction of white pulp
3439	Ccnd1/ Ikk2ca	normal	myeloma infiltrate
3443	Ccnd1/ Ikk2ca	diffuse myeloma infiltrate (80 %)	myeloma infiltrate
3444	Ccnd1/ Ikk2ca	myeloma infiltrate (60 %)	myeloma infiltrate
3459	Ccnd1/ Ikk2ca	myeloma infiltrate (70 %)	extensive myeloma infiltrate in red pulp
3468	Ccnd1/ Ikk2ca	myeloma infiltrate (50 %)	extensive myeloma infiltrate in red pulp

NOTE: Ccnd1/Ikk2ca mouse #3468 did not show ≥ 60 % myeloma infiltration in the histologic femur biopsy, but presented with high serum calcium (9.97 mg/dL) and low platelet (560 K/µL) levels reaching a myeloma-defining event (IMWG criteria (29)).

Tab. S4. Overview of dominant VDJ rearrangements of Ccnd1/Ikk2ca plasma cells determined by VDJ-PCR. Abbreviations: P/NP = productive/non-productive rearrangement; tissue = SPL (spleen section), F (femur section), BMPC (sorted CD138+TACI+ BM plasma cells); #SHM = amount of somatic hypermutation within VDJ rearrangement.

ID	genotype	PCR fragment	VDJ rearrangement	CDR3	P/NP	tissue	# SHM
3315	Ccnd1/ Ikk2ca	VHB-JH1	Ighv2-2*02; Ighd2-4*01; Ighj1*01	GCCAGAACTATGATTACGTACTTC GATGTC	P	F, BMPC	0 to 1
		VHB-JH3	Ighv2-9*02; Ighd2-10*02; Ighj2*01	GCCGCCCCCTACTATGGTAACGC CTGGTTTGCTTAC	P	F, BMPC	0 to 1
3433	Ccnd1/ Ikk2ca	VHE-JH1	Ighv5-1*01; Ighd1-2*01; Ighj2*01	TTGAGACAACATTAGGGGCTAC	NP	SPL, F, BMPC	1
		VHF-JH1	Ighv7-1*01; Ighd1-1*02; Ighj1*03	GCAAGAGATGATGGTTACTGGTA CTTCGATGTC	P	SPL, F, BMPC	1 to 2
3443	Ccnd1/ Ikk2ca	VHE-JH4	Ighv5-17*02; Ighd2-14*01; Ighj4*01	GCAACCTACTATAGGTACGACGG CTATGCTTTGGACTAC	P	SPL, F, BMPC	3 to 4
3459	Ccnd1/ Ikk2ca	VHB-JH1	Ighv2-6-7*01; Ighd2-4*01; Ighj3*01	GCCAGAGGAGGCAACTATGATTA CGACGGGTTTGCTTAC	P	BMPC	0
		VHG-JH4	Ighv9-3*01; Ighd4-1*01; Ighj4*01	GCAAGACGGGCTGGGACGGAGG CTATGGACTAC	P	BMPC	0 to 1
		VHG-JH4	Ighv9-3*02; Ighd1-1*01; Ighj4*01	GCAAGAAGGGTTTATTACTACGG TCCTTATGCTATGGACTAC	P	BMPC	0 to 1
3439	Ccnd1/ Ikk2ca	VHF-JH1	Ighv7-1*02; Ighd4-1*01; Ighj1*01	GCAAGAGATAACTGGGACTGGTA CTTCGATGTC	P	BMPC	1
3468	Ccnd1/ Ikk2ca	VHE-JH4	Ighv5-6-4*01; Ighd3-3*01; Ighj4*01	ACAAGAGATCTGGGGACGGAGG GGTATGCTATGGACTAC	P	SPL, BMPC	1
		VHB-JH4	Ighv2-9*02; Ighd2-14*01; Ighj4*01	GCCAGAGATATGTACGACTATGC TATGGACTAC	P	SPL, BMPC	0
		VHE-JH3	Ighv5-9-1*02; Ighd2-4*01; Ighj3*01	ACAAGAGATCATGATTACGACGG TTTGCTTAC	NP	SPL, BMPC	4
		VHA-JH3	Ighv1-19*01; Ighd1-1*01; Ighj3*01	GCCGTATTAATTACTACGGTACTA GAGGGGTTTGCTTAC	P	SPL, BMPC	15

Tab. S5. List of employed antibodies.

Reagents	Company	RR:ID	Catalog-Number	Method
α-B220-BV785	BioLegend	AB_11218795	103245	Flow Cytometry
α-CD19-BV650	BioLegend	AB_11204087	115541	Flow Cytometry
α-CD38 AlexaFluor700	Invitrogen	AB_657740	56-0381-82	Flow Cytometry
α-Fas-PECy7	BD Biosciences	AB_396768	557653	Flow Cytometry
α-IgG1-PE	BD Biosciences	AB_393553	550083	Flow Cytometry
α-CD138-APC	BioLegend	AB_10962911	142506	Flow Cytometry
α-TACI-PE	BD Biosciences	AB_647234	558410	Flow Cytometry
α-mouse Igκ-FITC	BD Biosciences	AB_393527	550003	Immunofluorescence
α-mouse Igλ-FITC	BD Biosciences	AB_394854	553434	Immunofluorescence
α-CD11c-PE	BioLegend	AB_313776	117307	Immunofluorescence
α-CD138-PE	BioLegend	AB_10916119	142504	Immunofluorescence
α-CD19-APC	BioLegend	AB_313647	115512	Immunofluorescence
α-B220-APC	BioLegend	AB_312997	103212	Immunofluorescence
α-mouse IgM-UNLB	Southern Biotech	AB_2794408	1070-01	ELISA
α-mouse IgM-BIO	Southern Biotech	AB_2737411	1020-08	ELISA/ELISPOT
α-mouse IgG-UNLB	Southern Biotech	AB_2794290	1030-01	ELISA
α-mouse IgG-AP	Southern Biotech	AB_2794293	1030-04	ELISA
α-mouse IgA-UNLB	Southern Biotech	AB_2314669	1040-01	ELISA
α-mouse IgA-BIO	Southern Biotech	AB_2794374	1040-08	ELISA/ELISPOT
α-mouse IgG1-BIO	Southern Biotech	AB_2794427	1071-08	ELISPOT
α-mouse IgG2a-BIO	Southern Biotech	AB_2794479	1080-08	ELISPOT
α-mouse IgG2b-BIO	Southern Biotech	AB_2794523	1090-08	ELISPOT
α-mouse IgG2c-BIO	Southern Biotech	AB_2794463	1078-08	ELISPOT
α-mouseIgG3-BIO	Southern Biotech	AB_2794575	1100-08	ELISPOT
α-mouse Igκ-UNLB	Southern Biotech	AB_2737431	1050-01	ELISPOT
α-mouse Igλ-UNLB	Southern Biotech	AB_2794389	1060-01	ELISPOT
Streptavidin-AP	MERCK		11089161001	ELISA
BCIP/NBT	Promega		S381C	ELISPOT
α-mouse IgM	SIGMA	AB_260700	M 8644	SPEP-Immunofixation
α-mouse IgG	SIGMA	AB_260466	M 1397	SPEP-Immunofixation
α–mouse IgA	SIGMA	AB_260464	M 1272	SPEP-Immunofixation
α-mouse Igκ	NOVUS Biologicals	AB_525186	NB7546	SPEP-Immunofixation
α-mouse Igλ	NOVUS Biologicals	AB_525259	NB7550	SPEP-Immunofixation
α-WHSC1/NSD2	abcam	AB_1310816	ab75359	Immunoblot
α-Cyclin D1	Cell Signaling	AB_2228523	2922	Immunoblot

Tab. S6. Overview of gene sets tested in the GSEA.

Gene set	Reference	# genes w/ mouse ensembl annotation
MM_signature_UP	Zhan et al., 2002; Table 5 + Lopez-Corral et al., 2014; Table S4	49 (38 + 11)
MM_signature_DOWN	Zhan et al., 2002; Table 4 + Lopez-Corral et al., 2014; Table S4	81 (26 + 55)
Gutierrez_WM	Gutierrez et al., 2007; Table 4	33
Gutierrez_MM	Gutierrez et al., 2007; Table 3	8
Bergsagel_11q13_UP	Bergsagel et al., 2005; Suppl. Table "MM 11q13 genes"	342
Bergsagel_MMSET_UP	Bergsagel et al., 2005; Suppl. Table "MM 4p16 genes"	230
Bergsagel_maf_UP	Bergsagel et al., 2005; Suppl. Table "MM maf genes"	236
Bergsagel_D1_UP	Bergsagel et al., 2005; Suppl. Table "MM D1 genes"	410
Bergsagel_D2_UP	Bergsagel et al., 2005; Suppl. Table "MM D2 genes"	150
Zhan_CD-1_UP	Zhan et al., 2006; Table S2; subgroup CD-1	34
Zhan_CD-1_DOWN	Zhan et al., 2006; Table S3; subgroup CD-1	31
Zhan_CD-2_UP	Zhan et al., 2006; Table S2; subgroup CD-2	35
Zhan_CD-2_DOWN	Zhan et al., 2006; Table S3; subgroup CD-2	33
Zhan_MMSET_UP	Zhan et al., 2006; Table S2; subgroup MS	33
Zhan_MMSET_DOWN	Zhan et al., 2006; Table S3; subgroup MS	28
Zhan_MF_UP	Zhan et al., 2006; Table S2; subgroup MF	35
Zhan_MF_DOWN	Zhan et al., 2006; Table S3; subgroup MF	31
Zhan_HP_UP	Zhan et al., 2006; Table S2; subgroup HP	31
Zhan_HP_DOWN	Zhan et al., 2006; Table S3; subgroup HP	34
Zhan_LB_UP	Zhan et al., 2006; Table S2; subgroup LB	35
Zhan_LB_DOWN	Zhan et al., 2006; Table S3; subgroup LB	25
Zhan_PR_UP	Zhan et al., 2006; Table S2; subgroup PR	34
Zhan_PR_DOWN	Zhan et al., 2006; Table S3; subgroup PR	59
Broyl_CD-1_UP	Broyl et al., 2010; Table S5; Cluster CD1 top up-regulated (50)	29
Broyl_CD-1_DOWN	Broyl et al., 2010; Table S5; Cluster CD1 top down-regulated (9)	5
Broyl_CD-2_UP	Broyl et al., 2010; Table S5; Cluster CD2 top up-regulated (50)	24
Broyl_CD-2_DOWN	Broyl et al., 2010; Table S5; Cluster CD2 top down-regulated (50)	20
Broyl_CTA_UP	Broyl et al., 2010; Table S5; Cluster CTA top up-regulated (50)	30
Broyl_CTA_DOWN	Broyl et al., 2010; Table S5; Cluster CTA top down-regulated (50)	31
Broyl_NFkB_UP	Broyl et al., 2010; Table S5; Cluster NFkB top up-regulated (50)	28
Broyl_NFkB_DOWN	Broyl et al., 2010; Table S5; Cluster NFkB top down-regulated (50)	39
Broyl_HY_UP	Broyl et al., 2010; Table S5; Cluster HY top up-regulated (50)	28
Broyl_HY_DOWN	Broyl et al., 2010; Table S5; Cluster HY top down-regulated (50)	28
Broyl_PRL3_UP	Broyl et al., 2010; Table S5; Cluster PRL3 top up-regulated (18)	11
Broyl_PRL3_DOWN	Broyl et al., 2010; Table S5; Cluster PRL3 top down-regulated (9)	6
Broyl_PR_UP	Broyl et al., 2010; Table S5; Cluster PR top up-regulated (50)	34
Broyl_PR_DOWN	Broyl et al., 2010; Table S5; Cluster PR top down-regulated (50)	31
Broyl_MF_UP	Broyl et al., 2010; Table S5; Cluster MF top up-regulated (50)	29

Broyl_MF_DOWN	Broyl et al., 2010; Table S5; Cluster MF top down-regulated (50)	24
Broyl_MMSET_UP	Broyl et al., 2010; Table S5; Cluster MS top up-regulated (50)	25
Broyl_MMSET_DOWN	Broyl et al., 2010; Table S5; Cluster MS top down-regulated (50)	26
Broyl_Myeloid_UP	Broyl et al., 2010; Table S5; Cluster Myeloid top up-regulated (50)	17
Broyl_Myeloid_DOWN	Broyl et al., 2010; Table S5; Cluster Myeloid top down-regulated (40)	28

SI References

1. K. Schmidt, *et al.*, B-Cell-Specific Myd88 L252P Expression Causes a Premalignant Gammopathy Resembling IgM MGUS. *Front. Immunol.* **11** (2020).
2. M. Peitz, K. Pfannkuche, K. Rajewsky, F. Edenhofer, Ability of the hydrophobic FGF and basic TAT peptides to promote cellular uptake of recombinant Cre recombinase: A tool for efficient genetic engineering of mammalian genomes. *PNAS* **99**, 4489–4494 (2002).
3. T. Nojima, *et al.*, In-vitro derived germinal centre B cells differentially generate memory B or plasma cells in vivo. *Nat. Commun.* **2**, 1–11 (2011).
4. D. Krappmann, *et al.*, Molecular mechanisms of constitutive NF-kB/Rel activation in Hodgkin/ Reed-Sternberg cells. *Oncogene* **18**, 943–953 (1999).
5. A. Ehlich, V. Martin, W. Müller, K. Rajewsky, Analysis of the B-cell progenitor compartment at the level of single cells. *Curr. Biol.* **4**, 573–583 (1994).
6. D. P. Calado, *et al.*, Constitutive Canonical NF-κB Activation Cooperates with Disruption of BLIMP1 in the Pathogenesis of Activated B Cell-like Diffuse Large Cell Lymphoma. *Cancer Cell* **18**, 580–589 (2010).
7. S. L. Rosales, *et al.*, "A Sensitive and Integrated Approach to Profile Messenger RNA from Samples with Low Cell Numbers BT - Type 2 Immunity: Methods and Protocols" in R. L. Reinhardt, Ed. (Springer New York, 2018), pp. 275–302.
8. R. Patro, G. Duggal, M. I. Love, R. A. Irizarry, C. Kingsford, Salmon provides fast and bias-aware quantification of transcript expression. *Nat. Methods* **14**, 417–419 (2017).
9. C. Soneson, M. I. Love, M. D. Robinson, Differential analyses for RNA-seq: transcript-level estimates improve gene-level inferences. *F1000Research* **4**, 1–19 (2016).
10. M. I. Love, W. Huber, S. Anders, Moderated estimation of fold change and dispersion for RNA-seq data with DESeq2. *Genome Biol.* **15**, 1–21 (2014).
11. F. Zhan, *et al.*, Global gene expression profiling of multiple myeloma, monoclonal gammopathy of undetermined significance, and normal bone marrow plasma cells. *Blood* **99**, 1745–1757 (2002).
12. L. López-Corral, *et al.*, Transcriptome analysis reveals molecular profiles associated with evolving steps of monoclonal gammopathies. *Haematologica* **99**, 1365–1372 (2014).
13. N. C. Gutiérrez, *et al.*, Gene expression profiling of B lymphocytes and plasma cells from Waldenström's macroglobulinemia: Comparison with expression patterns of the same cell counterparts from chronic lymphocytic leukemia, multiple myeloma and normal individuals. *Leukemia* **21**, 541–549 (2007).
14. P. L. Bergsagel, *et al.*, Cyclin D dysregulation: An early and unifying pathogenic event in multiple myeloma. *Blood* **106**, 296–303 (2005).
15. F. Zhan, *et al.*, The molecular classification of multiple myeloma. *Blood* **108**, 2020–2028 (2006).
16. A. Broyl, *et al.*, Gene expression profiling for molecular classification of multiple myeloma in newly diagnosed patients. *Blood* **116**, 2543–2553 (2010).
17. J. Weiner, T. Domaszewska, tmod: an R package for general and multivariate enrichment analysis. *PeerJ Prepr.*, 1–9 (2016).
18. J. Weiner, Feature Set Enrichment Analysis for Metabolomics and Transcriptomics (2020) (August 26, 2021).
19. G. Yu, enrichplot: Visualization of Functional Enrichment Result. (2021) (August 26, 2021).
20. S. Casola, *et al.*, Tracking germinal center B cells expressing germ-line immunoglobulin g1 transcripts by conditional gene targeting. *PNAS* **103**, 7396–7401 (2006).
21. S. Chen, Y. Zhou, Y. Chen, J. Gu, Fastp: An ultra-fast all-in-one FASTQ preprocessor. *Bioinformatics* **34**, i884–i890 (2018).
22. H. Li, Aligning sequence reads, clone sequences and assembly contigs with BWA-MEM. arXiv [Preprint] (2013). https://doi.org/10.48550/arXiv.1303.3997.
23. G. A. Van der Auwera, B. D. O'Connor, *Genomics in the Cloud: Using Docker, GATK, and*

WDL in Terra (O'Reilly Media, Inc., 2020).
24. D. Benjamin, *et al.*, Calling Somatic SNVs and Indels with Mutect2. bioRxiv [Preprint] (2019). https://doi.org/10.1101/861054.
25. A. Wilm, *et al.*, LoFreq: A sequence-quality aware, ultra-sensitive variant caller for uncovering cell-population heterogeneity from high-throughput sequencing datasets. *Nucleic Acids Res.* **40**, 11189–11201 (2012).
26. Y. Fan, *et al.*, MuSE: accounting for tumor heterogeneity using a sample-specific error model improves sensitivity and specificity in mutation calling from sequencing data. *Genome Biol.* **17**, 178 (2016).
27. S. T. Sherry, *et al.*, dbSNP: the NCBI database of genetic variation. *Nucleic Acids Res.* **29**, 308–311 (2001).
28. E. Talevich, A. H. Shain, T. Botton, B. C. Bastian, CNVkit: Genome-Wide Copy Number Detection and Visualization from Targeted DNA Sequencing. *PLoS Comput. Biol.* **12** (2016).
29. S. V. Rajkumar, *et al.*, International Myeloma Working Group updated criteria for the diagnosis of multiple myeloma. *Lancet Oncol.* **15**, e538–e548 (2014).